Biophysical Chemistry 147 (2010) 81–86

Contents lists available at ScienceDirect

Biophysical Chemistry

journal homepage: http://www.elsevier.com/locate/biophyschem

Short Communication

Real-time observation of model membrane dynamics induced by Alzheimer's amyloid beta

Masamune Morita, Mun'delanji Vestergaard *, Tsutomu Hamada, Masahiro Takagi

School of Materials Science, Japan Advanced Institute of Science and Technology, 1-1 Asahidai, Nomi City, Ishikawa, 923-1292, Japan

ARTICLE INFO

Article history:
Received 26 October 2009
Received in revised form 11 December 2009
Accepted 13 December 2009
Available online 16 December 2009

Keywords:
Amyloid beta
Alzheimer's
Aggregation species
Membrane transformation
Membrane fluctuation

ABSTRACT

Amyloid beta (Aβ) has been strongly implicated in inducing neurotoxicity in the pathology of Alzheimer's disease (AD). However, the underlying mechanisms remain unknown. In this study, we examined, in real-time, the spatio-temporal changes in individual model membranes induced by the presence of different Aβ-40 molecular assemblies (species). We used cell-sized lipid vesicles to enable the direct observation of these changes. We found three significantly different membrane-transformation pathways. We characterized the biophysical mechanisms behind these transformations in terms of the change in inner vesicle volume and surface area. Oligomeric Aβ exhibited the highest tendency to cause membrane fluctuation and transformations. Interestingly, mature fibrils, which are often considered inert species, also induced profound membrane changes. Furthermore, we imaged the localization of pre-fibrillar species on membranes. The real-time observation of these morphological transformations, which can be missed in a discretised analysis, may help to unlock the mechanisms of AD's Aβ-induced neuro-degeneration.

1. Introduction

Alzheimer's disease (AD) is an age-related cognitive impairment, mainly characterized by formation of senile (amyloid) plaques and neurofibrillary tangles in the brain of AD individuals, involving amyloid beta (Aβ) peptides and tau protein, respectively [1–3]. The mechanism by which the two exert neurotoxicity is not well understood. The current work investigates possible mechanisms for Aβ-mediated membrane malfunction. Aβ-peptides are natively unfolded protein but aggregates into β-sheet structure of ordered fibrils [4–6]. Fibril formation proceeds from nucleation, via oligomers to mature fibrils. A detailed account of the pathways for Aβ oligomerisation and assembly can be found in a review by Murphy [7]. Soluble oligomers are a common intermediate in the pathway for fibril formation, and some have held these intermediates as the most toxic species of amyloid related to neurodegenerative disease [8,9]. Others hold the view that fibrils are the principal triggers of neuronal cell toxicity or disorder [5,10–12].

Aβ-induced neuronal cell toxicity has been reported to be due to (i) pore formation, (ii) the disruption of ionic channels that could affect calcium homeostasis, and (iii) receptor binding [3,13]. Thus, the actual mechanism of Aβ-induced neuronal cell toxicity remains unclear. There has been extensive research on the role of Aβ in AD covering interactions between Aβ and lipids [14]. Lipid and cholesterol compositions have been reported to affect oligomerisation and reverse ('backward') oligomerisation [15]. Small and large lipid vesicles (< μm) have also been exploited to study the influence of lipid bilayer on Aβ-peptide assembly [16]. As is perhaps apparent, all these studies have concentrated on the effect of Aβ oligomerisation and assembly. From the results, an inference has been drawn on how different Aβ molecular species cause neurotoxicity. The deductions have been made mainly using histochemical dyes [15], and not direct real-time observation of what may be taking place to the biological or lipid vesicles used. The studies on the interaction between Aβ-peptides and lipid vesicles have concentrated in the how the composition of the membranes affects the peptides. In particular, how levels of cholesterol and different lipid compositions in a given model membrane, affect oligomerisation and assembly of the peptides [17,18].

Our focus is different in that we are directly studying membrane responses to the presence of Aβ-peptides. Specifically, we used cell-sized (>10 μm) model membranes to directly observe spatio-temporal changes in individual vesicles. These biomimetic membranes enable the researcher to manipulate a 'biological' micro-vesicle under a controlled environment [19]. In this study, using fluorescence-labeled Aβ-40 (Hilyte Fluor™488-β-Amyloid(1–40)), we successfully imaged the localization of pre-fibrillar Aβ species on the membrane surface, and the temporal dependence of this peptide–membrane lipid association. Further, we investigated the interaction of different oligomeric species of the Aβ peptide with lipid vesicles, observing membrane stability in terms of fluctuations and morphological changes in real-time, using a simple phase-contrast microscope. We captured three different

* Corresponding author. Tel.: +81 761 51 1598; fax: +81 761 51 1650.
E-mail addresses: s0830078@jaist.ac.jp (M. Morita), munde@jaist.ac.jp (M. Vestergaard), t-hamada@jaist.ac.jp (T. Hamada), takagi@jaist.ac.jp (M. Takagi).

0301-4622/$ – see front matter © 2009 Elsevier B.V. All rights reserved.
doi:10.1016/j.bpc.2009.12.004

pathways to membrane morphological changes, both of which followed membrane fluctuation. We propose that this alternative way of looking at Alzheimer's Aβ interaction with membranes may provide new biophysical mechanisms with ways in which Aβ induces membrane damage.

2. Materials and methods

2.1. Reagents and amyloid beta-peptide

Amyloid β-40 (trifluoroacetate salt) was purchased from Peptide Institute Inc., (Osaka, Japan), 1,2-Dioleoyl-sn-Glycero-3-Phosphocholine (DOPC) was obtained from Avanti Polar Lipids, mica disks were from Furuuchi Chemical Co. (Tokyo, Japan), and Amyloid β-40 HiLyte Fluor™ 488-labeled, Anaspec. All other chemicals were purchased from Wako Pure Chem. Co. (Japan).

2.2. Preparation of Giant Unilamellar Vesicles (GUV) and observation using an optical microscope

Giant liposomes were prepared by gentle hydration method [20,21]. DOPC lipid was dissolved in chloroform/methanol (1:1 v/v) mixture. DOPC solution was transferred into a glass tube and gently dried using a stream of nitrogen gas, to produce a thin lipid film. The thin film was subsequently dried under vacuum overnight, and was hydrated with ultrapure Milli Q (18 Ω) for 3 h at 37 °C. The final lipid concentration was 0.5 mM. Four μL of this vesicle solution was placed in a silicon well (100 nm) on a glass slide, and covered with a cover slip. Examination was carried out using a phase-contrast microscope (Olympus BX-51, Japan). The silicon well and the cover slip ensured that evaporation of the solution did not occur over the duration of the experiment.

2.3. Interaction of Aβ-40 with GUVs

Amyloid β was incubated at 37 °C in 20 mM Tris buffer, pH 7.4 at 80 μM concentration for various incubation periods. Alternatively, we could have used phosphate buffer saline, but chose Tris in order to maintain similar conditions to related previous work [22–24], thus enabling direct relationships to be drawn. It is well known that amyloid beta assembly is influenced by incubation conditions [25]. After incubation, Aβ was introduced to lipid vesicles at a final concentration of 2 μM in 0.5 mM Tris buffer, by dilution in Milli Q water. Tris buffer at >0.5 mM ionic strength interfered with membrane stability. Immediately after addition, the vial containing the lipid vesicles and Aβ were mixed gently by tapping. Observation of the vesicular dynamics was within 2 min of peptide introduction to the lipid vesicles. Real-time observation of Aβ-40–vesicle interaction was observed as above, for a total period of 20 min.

2.4. Procedure for preparation of the osmotic stress environment

DOPC lipid vesicles and glucose solution were gently mixed by soft tapping. The final concentration of lipid was 0.25 mM, and the difference in the molar concentration of glucose across the bilayer membrane was 1.0 mM. Four μL of this glucose:lipid vesicle solution was placed on a glass slide and examined using a phase-contrast microscope (Olympus BX-51, Japan).

2.5. Association and localization of Aβ-40 on GUVs

HiLyte Fluor™ 488-labeled Aβ-40 and Aβ-40 was mixed 1:2 (mol ratio). Aβ-40 was added to lipid vesicles to a final concentration of 2 μM. Four μL of this solution was imaged using a confocal microscope (Olympus FV-1000, Japan).

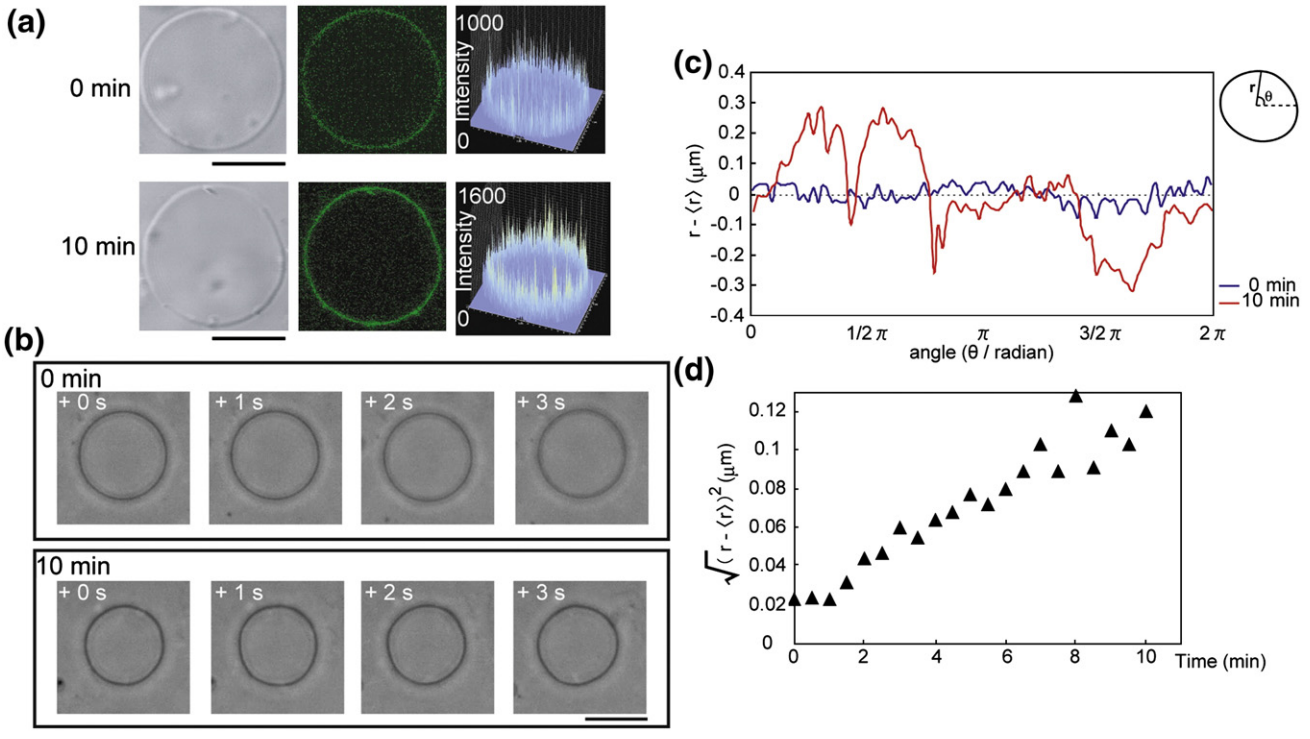

Fig. 1. Typical localization of fluorescent-labeled pre-fibrillar Aβ-40 (2 μM) on DOPC lipid vesicles Aβ-40 (80 μM) was incubated in 20 mM Tris buffer, pH 7.4 at 37 °C for 1 day ($n=5$) (a): differential interference image of the vesicle (left); fluorescence-labeled Aβ-40 (center); and fluorescence intensity of Aβ-40 (right) after 0 and 10 min of interaction. The phase-contrast microscopy image of membrane fluctuation 0 and 10 min after introduction of Aβ-40 to lipid vesicle (b). Degree of membrane fluctuation 0 and 10 min after introduction of Aβ-40 to lipid vesicle. Plotted the value of $(r-\langle r\rangle)$ in each θ ($\theta=2\pi/n$, $n=0, 1\ldots 100$) (c). Time dependence of membrane fluctuation after introduction of Aβ-40 to lipid vesicle. Calculated the value of $\langle \mathrm{sqr}(r-\langle r\rangle)^2\rangle_\theta$ ($\theta=2\pi/n$, $n=0, 1\ldots 100$) for time periods (0, 0.5, 1… 10 min) (d). The lag-time between addition of Aβ-40 and the actual observation is 2 min.

2.6. Imaging Amyloid β-40 assembly using atomic force microscopy (AFM)

Aβ-40 was taken out from incubation, and samples were diluted with Milli Q to a final concentration of 10 μM. Immediately after, the peptide was immobilized on clean mica disk (Furuuchi Chemical Co., Shinagawa, Tokyo, Japan). AFM images were obtained using an AFM unit (SPA400-SPI3800, Seiko Instruments Inc., Chiba, Japan) equipped with a calibrated 20 μm *xy*-scan and 10 μm *z*-scan range PZT-scanner and a silicon nitride tip (SI-DF40P, spring constant = 42 N/m, frequency resonance = 300 kHz, Seiko Instruments Inc.) was used for AFM imaging of samples. All AFM images were obtained in air in a dynamic force mode (DFM mode) at optimal force. All AFM operations were done in an automated moisture control box with 30–40% humidity at RT.

3. Results and discussion

3.1. Localization of amyloid beta on membrane surface

First, we incubated 80 μM Aβ-40 in 20 mM Tris, pH 7.4 (Tris) at 37 °C for various periods. Immediately after incubation, Aβ-40 (2 μM) was added to cell-sized lipid vesicles composed of dioleoyl-phosphatidylcholine (DOPC), and their interaction was observed in real-time. Pre-fibrillar Aβ localized on the membrane surface, and interacted with the vesicle (Fig. 1a). The localization was time-dependent. Fluctuation of the membrane was the first response to the presence of the Aβ-peptide, and its intensity increased with interaction time (Fig. 1b, c, d). Efforts towards attaining detailed time resolution data relating association time and degree of Aβ localization; and how this may relate to issues such as breach of membrane barrier and lipid recruitment are ongoing.

3.1. Membrane morphological changes induced by amyloid beta

We captured three distinct vesicular transformation pathways induced by different Aβ-40 species. Some vesicles did not show any changes in the presence of the peptide, while others exhibited fluctuations that culminated in shape changes (Fig. 2, and movies 1 and 2 in the Supplementary material). Some vesicles formed small sphero-stomatocytes (Fig. 2a), while others formed exo-tubes/-buds (Fig. 2b), and large sphero-stomatocytes (Fig. 2c), at the end of the vesicular transition. The effect of proteins and osmotic stress on membrane fluctuation, and/or morphology has been reported [26–28]. To gain a better understanding of the observed Aβ-induced morphological changes, we investigated the behavior of our membrane under osmotic stress. We observed membrane morphological transformations that culminated in a vesicle with a very small inner bud (Fig. S1), upon exposure to osmotic stress. The transformation induced by osmotic stress was very similar to the membrane dynamics pathway that culminated in formation of a small sphero-stomatocyte.

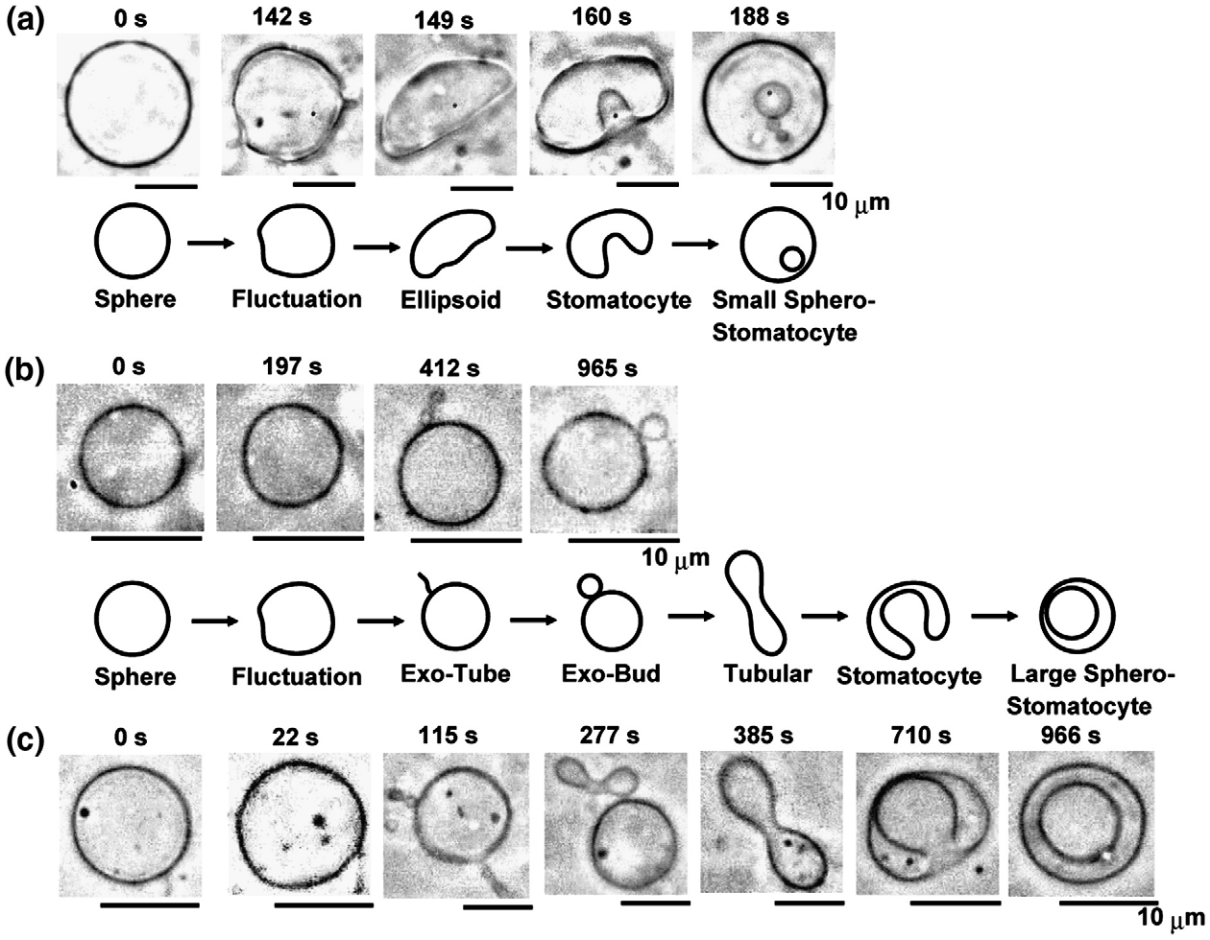

Fig. 2. Lipid vesicle transformation pathway in response to Aβ-40 (2 μM) added after 0–5 days incubation in 80 μM in 20 mM Tris buffer, pH 7.4 at 37 °C. We have coined the pathways: small sphero-stomatocyte (a), exo-tube/bud (b), and large sphero-stomatocyte (c).

3.3. Relationship between membrane destabilization and amyloid beta aggregation species

We established a relationship between the degree of Aβ assembly and membrane dynamic responses (Fig. 3, and Table S1 in the Supplementary material). Typical AFM images of Aβ showed different Aβ species, from small oligomeric to mature fibrils with increase in incubation period. Fig. 3a clearly reveals that the frequency of membrane instability (fluctuation and morphological changes), was the highest when Aβ was introduced to the membrane surface after 1 day of incubation. We refer to this species as oligomeric Aβ. Fig. 3b provides detailed information on the types of membrane instability induced by the different Aβ species. Oligomeric (Day 1) and proto-fibrillar Aβ (Days 2 and 3) species exhibited the most diverse range in membrane responses, with the oligomeric species giving the highest tendency to induce large sphero-stomatocytes. Large sphero-stomatocytes were formed only in response to addition of Aβ incubated for 1, 2 and 3 days. Our results (in terms of tendency to perturb the membrane and cause diverse morphological changes) are in line with reports that oligomeric (/proto-fibrillar/intermediate) Aβ species have been widely reported as the most toxic species [8,9].

3.4. Biophysical characterization of membrane morphological changes

We characterized the vesicular transformations in terms of the increase in excess surface area ξ [21]. The excess area, also called the reduced volume, is a dimensionless parameter that describes membrane morphology in terms of Helfrich bending energy, and is defined by the ratio of the membrane surface area and vesicular volume [29,30]. We calculated the surface area and volume changes just after addition of the peptide and just after inner bud formation. Fig. 4 shows the dimensionless excess area ξ of the obtained sphero-stomatocyte and the radius of the inner bud r divided by R_0 (initial vesicular radius) for the large (square) and small (triangular) sphero-stomatocyte vesicles (detailed calculation, table (Table S2) and graph for the reduced volume in the Supplementary material (Fig. S2)). The black line shows the relationship between the two variables under a constant surface area (A), and the gray line shows this relationship under a constant vesicular volume (V). The small sphero-stomatocyte vesicles fit on A-constant curve but not on the V-constant curve. The large sphero-stomatocyte vesicles do not fit on either curve. The graph reveals that the two membrane dynamics induced by Aβ are clearly different. The large sphero-stomatocyte vesicles showed an increase in surface area (35%, $n=7$), and a decrease in inner volume of 28%. The small sphero-stomatocyte vesicles showed hardly any change in surface area (0.2%, $n=10$), and a decrease in inner volume of 13%.

Engel et al. studied membrane damage by human islet amyloid polypeptide (IAPP) through fibril growth at the membrane, and not necessarily a particular IAPP species (fibrillar or pre-fibrillar) [31]. The same group had previously reported that membrane barrier was compromised due to uptake of lipids from the lipid bilayer during amyloid fibril formation [32]. Our current work shows that different Aβ species induced membrane fluctuation, and morphological changes to different extents (Fig. 3). We show that oligomeric species has the most effect, followed by proto-fibrillar species. Engel et al., also showed a similar change in membrane shape that we captured, which later regained the original shape [31]. The interaction of rigid fibrils with a soft DOPC membrane may change the spontaneous curvature of the membrane to initiate membrane fluctuation. Obtained excess area can cause vesicular transformation as the membrane regains a favorable low-energy state [21,30]. In addition, we captured changes in the vesicle interior. The formation of an inner bud could influence the spatial localization of membrane proteins such as receptors. The slow membrane dynamics caused an increase

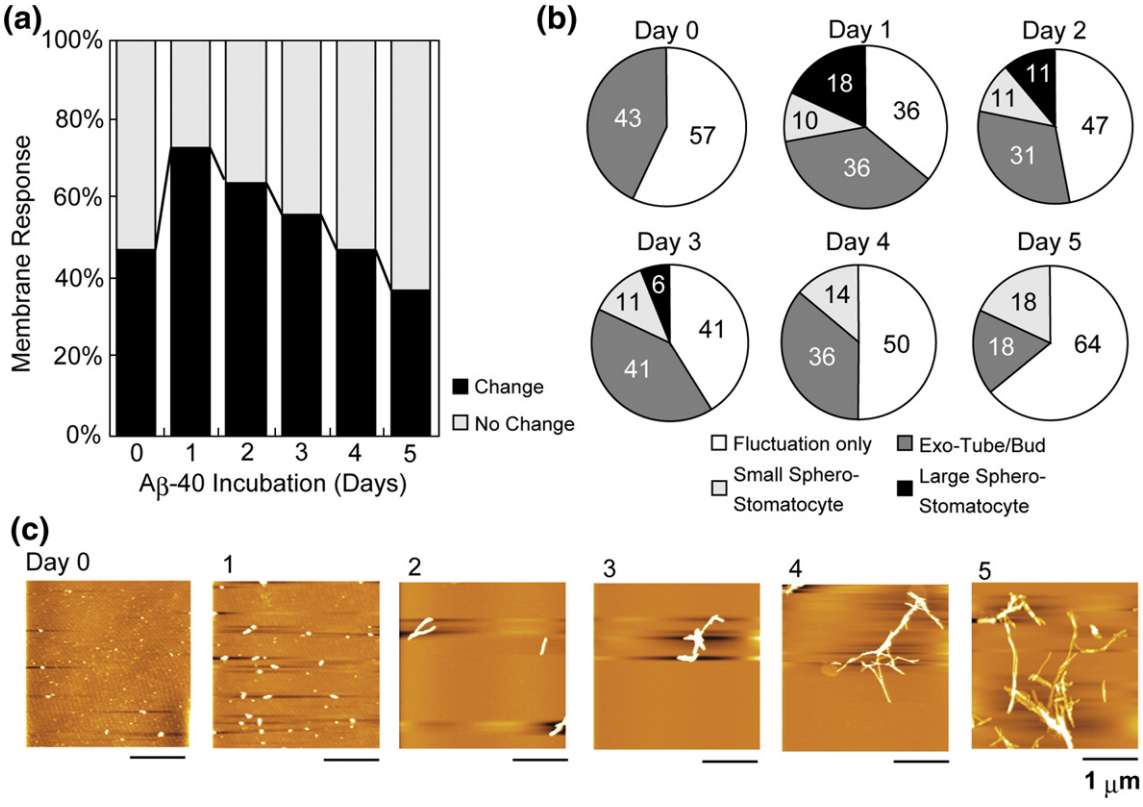

Fig. 3. Response of DOPC vesicles upon addition of Aβ-40 incubated for the indicated time periods. ($n=30$) (a). Detailed description and breakdown of how vesicles were destabilized by the peptide incubated at the time periods shown (b). Typical atomic force microscopy images of Aβ-40 (10 μM) after incubation shows small oligomeric (Day 0), oligomeric (Day 1), proto-fibrillar (Days 2 and 3), and mature fibrillar (Days 4 and 5) species (c). Bar represents 1 μm. Aβ-40 was incubated at 80 μM in 20 mM Tris buffer, pH 7.4, at 37 °C for 0, 1, 2, 3, 4, and 5 days).

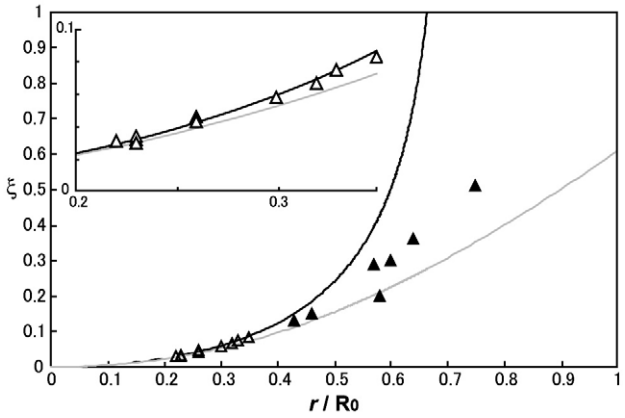

Fig. 4. Dimensionless excess area ξ of transformed liposomes plotted against the radius of the inner bud *r* for the small sphero-stomatocyte (white triangular) and large sphero-stomatocyte (black triangular). Surface area constant (*A*, black line) and inner volume constant (*V*, gray line) are shown. Vesicles lying left of the *A* and *V* curves had a decrease in value, those on the curves exhibited no change, and those right of the curves had an increase in the value. The value being either surface area or inner volume.

in surface area. We propose that this increase in surface area could be due to incorporation of oligomeric Aβ into the membrane bilayer. The affinity of Aβ and Amylin (IAPP) to lipids is reported [31–33]. Using raft-exhibiting lipid vesicles, Aβ-peptide (Aβ-40) has been reported to localize within the non-raft domains [24]. Oligomeric Aβ species, due to natural affinity to lipids, recruited free lipids and small vesicles (micelles) into the mother vesicle. The uptake of lipids by amyloids from vesicles has been reported [32]. With obvious localization of Abeta on the membrane surface as we have shown, we lean more on the incorporation of the peptide into the vesicular surface, as the main reason for the increased surface area. Since DOPC is a zwitterionic lipid, its interactions with Aβ were hydrophobic-driven. Arispe et al., first reported pore formation of Aβ peptide as one of the main mechanisms for Aβ-induced toxicity [34]. Since then, there have been several reports on how the peptide breaches the membrane barrier [31,32,35]. From our results, we cannot confirm nor refute this. However, in view of these reports, and our results, we propose that formation of sphero-stomatocytes could influence the spatial localization of membrane proteins such as receptors. The increase in surface area in vesicles which changed into large sphero-stomatocytes could disturb the packing of lipid molecules in the bilayer. As a result, the packing would become sub-optimal, creating small pores [36].

In conclusion, this study has provided a real-time demonstration that Aβ-40 may cause membrane damage by changing membrane morphology. Using cell-sized lipid vesicles, we found that the presence of Aβ assembled species induce membrane fluctuations. This instability sometimes culminates in one of the three membrane-transformation pathways. In this study, we used a simple homogenous DOPC membrane system in order to ascertain that the observed changes were due to interaction between the zwitterionic lipid and Aβ. A heterogenous raft-exhibiting model membrane system would provide information that could be closely related to the physiology environment. Indeed, we have already investigated the localization of the peptide in a heterogenous raft-exhibiting membrane system, as a first step towards detection of membrane responses to the presence of Aβ. The peptide preferentially associated with the non-raft region of the lipid vesicle, composed mainly of DOPC lipid. [24]. A biophysical characterization of sphero-stomatocyte terminating pathways showed changes in inner volume associated with both pathways, and a surface area increase associated with only one of the pathways. We have made initial attempts to relate these differences with the degree of Aβ assembly.

Acknowledgements

Technical assistance of membrane fluctuation analysis from Dr. Masaomi Hatakeyama is greatly appreciated. M.V. gratefully acknowledges financial support from the Japan Society for the Promotion of Science (JSPS). This work was supported by a KAKENHI Grant-in-Aid for Scientific Research (B) (No. 20360370) from JSPS and by a grant for studies on Priority Areas "Bio Manipulation" and "Soft Matter Physics" from the Ministry of Education, Culture, Sports, Science and Technology of Japan.

Appendix A. Supplementary data

Supplementary data associated with this article can be found, in the online version, at doi:10.1016/j.bpc.2009.12.004.

References

[1] M. Mattson, Pathways towards and away from Alzheimer's disease, Nature 430 (2004) 631–639.
[2] D.J. Selkoe, Alzheimer's disease results from the cerebral accumulation and cytotoxicity of amyloid β-protein, J. Alzheimer's Dis. 3 (2001) 75–80.
[3] D.M. Walsh, D.J. Selkoe, Deciphering the molecular basis of memory failure in Alzheimer's disease, Neuron 44 (2004) 181–193.
[4] C.A. Ross, M.A. Poirier, Protein aggregation and neurodegenerative disease, Nat. Med. 10 (2004) S10–S17.
[5] M. Stefani, C.M. Dobson, Protein aggregation and aggregate toxicity: new insights into protein folding, misfolding diseases and biological evolution, J. Mol. Med. 81 (2003) 678–699.
[6] J.C. Rochet, P.T. Lansbury, Amyloid fibrillogenesis: themes and variations, Curr. Opin. Struct. Biol. 10 (2000) 60–68.
[7] R.M. Murphy, M.M. Palitto, Probing the kinetics of β-amyloid self-association, J. Struct. Biol. 130 (2000) 109–120.
[8] M. Bucciantini, E. Giannoni, F. Chiti, F. Baroni, L. Formigli, J.S. Zurdo, N. Taddei, G. Ramponi, C.M. Dobson, M. Stefani, Inherent toxicity of aggregates implies a common mechanism for protein misfolding diseases, Nature 416 (2002) 507–511.
[9] R. Kayed, E. Head, J.L. Thomson, T.M. McIntire, S.C. Milton, C.W. Cotman, C.G. Glabe, Common structure of soluble amyloid oligomers implies common mechanism of pathogenesis, Science 300 (2003) 486–489.
[10] J. Tsai, J. Grutzendler, K. Duff, W.B. Gan, Fibrillar amyloid deposition leads to local synaptic abnormalities and breakage of neuronal branches, Nat. Neurosci. 7 (2004) 1181–1183.
[11] A. Lorenzo, B.A. Yankner, Amyloid fibril toxicity in Alzheimer's disease and diabetes, Ann. N. Y. Acad. Sci. 777 (1996) 89–95.
[12] E.A. Grace, C.A. Rabiner, J. Busciglio, Characterization of neuronal dystrophy induced by fibrillar amyloid β: implications for Alzheimer's disease, Neuroscience 114 (2002) 265–273.
[13] J. Lauren, D.A. Gimbel, H.B. Nygaard, J.W. Gilbert, S.M. Strittmatter, Cellular prion protein mediates impairment of synaptic placsticity by amyloid-β oligomers, Nat. Lett. 457 (2001) 1128–1138.
[14] A. Chauhan, I. Ray, V.P.S. Chauhan, Interaction of amyloid beta-protein with anionic phospholipids: possible involvement of Lys28 and C-terminus aliphatic amino acids, Neurochem. Res. 25 (2000) 423–429.
[15] I.C. Martins, I. Kuperstein, H. Wilknson, E. Maes, M. Vanbrabant, M. Jonckheere, P. Van Gelder, D. Hartmann, R. D'Hooge, B. De Strooper, J. Schymkowitz, F. Rousseau, Lipids revert inert Aβ amyloid fibrils to neurotoxic protofibrils that affect learning in mice, Eur. Mol. Biol. J. 27 (2008) 224–233.
[16] A. Kakio, S. Nishimoto, K. Yanagisawa, Y. Kozutsumi, K. Matsuzaki, Cholesterol-dependent formation of GM1 ganglioside-bound amyloid β-protein, an endogenous seed for Alzheimer amyloid, J. Biol. Chem. 276 (2001) 24985–24990.
[17] L. Rojo, M.K. Sjoberg, P. Hernandez, C. Zambrano, R.B. Maccioni, Roles of cholesterol and lipids in the etiopathogenesis of Alzheimer's disease, J. Biomed. Biotechnol. (2006) 1–17.
[18] M. Vestergaard, T. Hamada, M. Morita, M. Takagi, Cholesterol, lipids, amyloid beta, and Alzheimer's. Curr. Alzheimer Res. (in press).
[19] M. Vestergaard, T. Hamada, M. Takagi, Using model membranes for the study of amyloid beta:lipid interactions and neurotoxicity, Biotechnol. Bioeng. J. 99 (2008) 753–763.
[20] T. Hamada, Y. Miura, K. Ishii, S. Araki, K. Yoshikawa, M. Vestergaard, M. Takagi, Dynamic processed in endocytic transformation of a raft-exhibiting giant vesicle, J. Phys. Chem. B. 111 (2007) 10853–10857.
[21] K. Ishii, T. Hamada, M. Hatakeyama, R. Sugimoto, T. Nagasaki, M. Takagi, Reversible control of exo- and endo-budding transitions in a photo-sensitive membrane, ChemBioChem 10 (2009) 251–256.
[22] M. Vestergaard, K. Kerman, M. Saito, N. Nagatani, Y. Takamura, E. Tamiya, A rapid label-free electrochemical detection and kinetic study of Alzheimer's amyloid beta aggregation, J. Am. Chem. Soc. 127 (2005) 11892–11893.
[23] M. Vestergaard, T. Hamada, M. Saito, Y. Yajima, M. Kudou, E. Tamiya, M. Takagi, Detection of Alzheimer's amyloid beta aggregation by capturing molecular trails of individual assemblies, Biochem. Biophys. Res. Commun. 377 (2008) 725–728.

[24] T. Hamada, M. Morita, Y. Kishimoto, Y. Komatsu, M. Vestergaard, M. Takagi, Biomimetic microdroplet membrane interface: detection of the lateral localization of amyloid beta peptides, J. Phys. Chem. Lett. 1 (2010) 170–173.
[25] K. Matsuzaki, Physicochemical interactions of amyloid b-peptide with lipid bilayers, Biochim. Biophys. Acta 1768 (2007) 1935–1942.
[26] T. Hamada, Y.T. Sato, T. Nagasaki, K. Yoshikawa, Reversible photo-switching in a cell-sized vesicle, Langmuir 21 (2005) 7626–7628.
[27] A. Viallat, J. Dalous, M. Abkarian, Giant lipid vesicles filled with a gel: shape stability induced by osmotic shrinkage, Biophys. J. 86 (2004) 2179–2187.
[28] F. Nomura, T. Inaba, S. Ishikawa, M. Nagata, S. Takashi, H. Hotani, K. Takiguchi, Microscopic observations reveal that fusogenic peptides induce liposome shrinkage prior to membrane fusion, Proc. Natl. Acad. Sci. U. S. A. 101 (2004) 3420–3425.
[29] H.G. Dobereiner, Properties of giant vesicles, Curr. Opin. Colloid Interface Sci. 5 (2000) 251–255.
[30] U. Seifert, K. Berndl, R. Lipowsky, Shape transformations of vesicles: phase diagram for spontaneous- curvature and bilayer-coupling models, Phys. Rev. A 44 (1991) 1182–1202.
[31] M.F. Engel, L. Khemtemourian, C.C. Kleijer, H.H. Meedijk, J. Jacobs, E.J. Verkleij, B. de Kruijff, J.A. Killian, J.W.M. Höppener, Membrane damage by human islet amyloid polypeptide through fibril growth at the membrane, Proc. Natl. Acad. Sci. U. S. A. 105 (2008) 6033–6038.
[32] E. Sparr, M. Engel, D. Sakharov, M. Sprong, J. Jacobs, B. de Kruijff, J.W.M. Höppener, J.A. Killian, Islet amyloid polypeptide-induced membrane leakage involves uptake of lipids by forming amyloid fibers, FEBS Lett. 577 (2004) 117–120.
[33] H. Zhao, E.K.J. Tuominen, P.K.J. Kinnunen, Formation of amyloid fibers triggered by phosphatidylserine-containing membranes, Biochemistry 42 (2004) 10302–10307.
[34] N. Arispe, E. Rojas, H.B. Pollard, Alzheimer's disease amyloid b-protein forms channels in bilayer membranes. Blockage by tromethamine and aluminium, Proc. Natl. Acad. Sci. U. S. A. 90 (1993) 567–571.
[35] J.H. Zheng, R. Nussinov, Models of beta-amyloid ion channels in the membrane suggest that channel formation in the bilayer is a dynamic process, Biophys. J. 96 (2007) 1938–1949.
[36] R. Friedman, R. Pellarin, A. Caflish, Amyloid aggregation on lipid bilayers and its impact on membrane permeability, I, Mol. Biol. 387 (2009) 407–415.